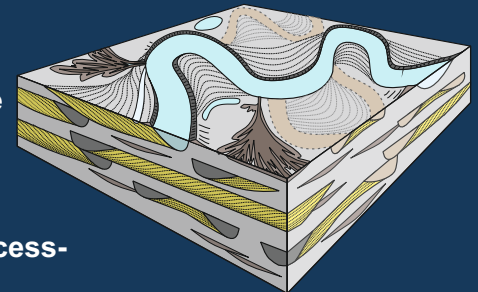
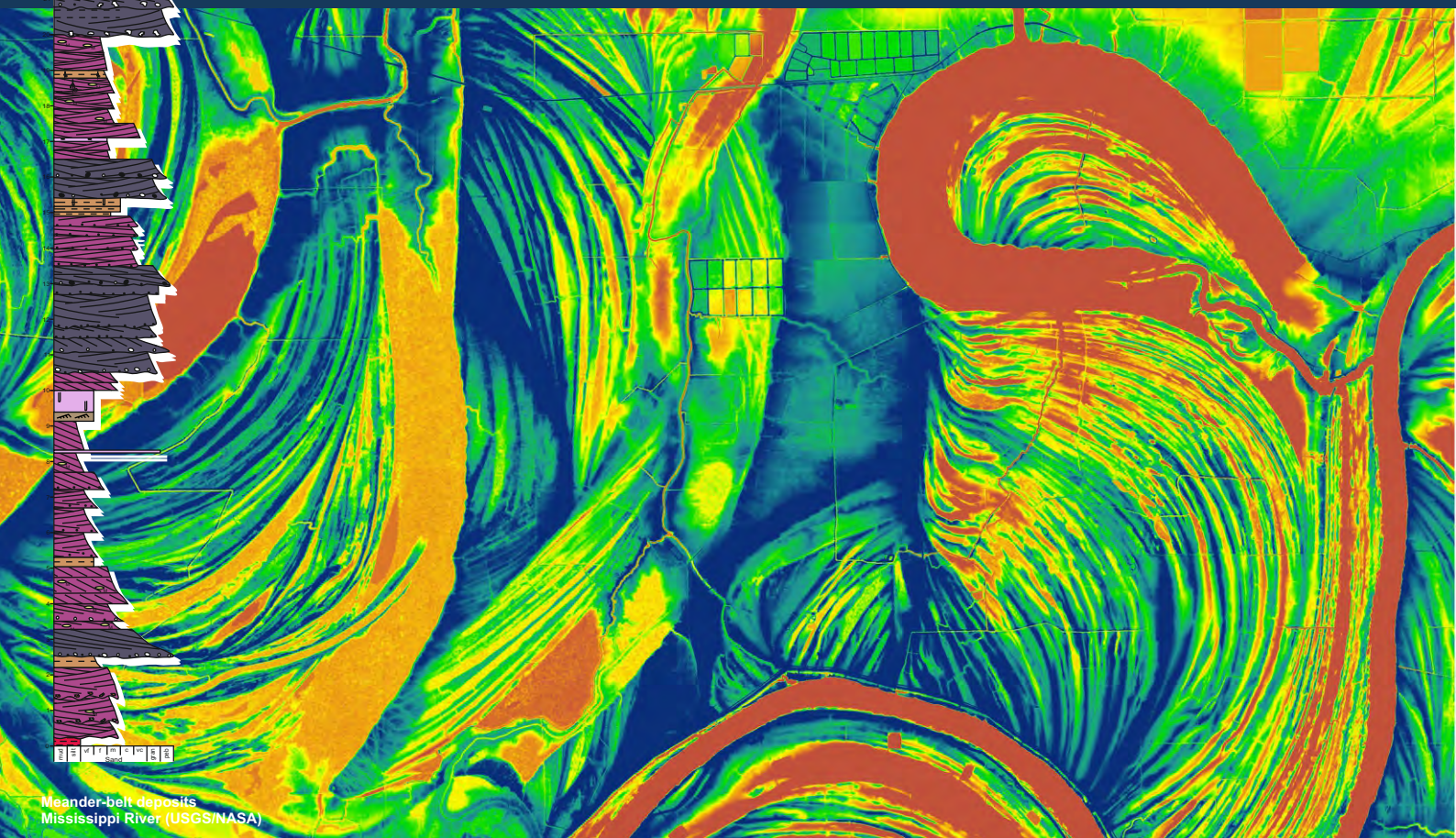
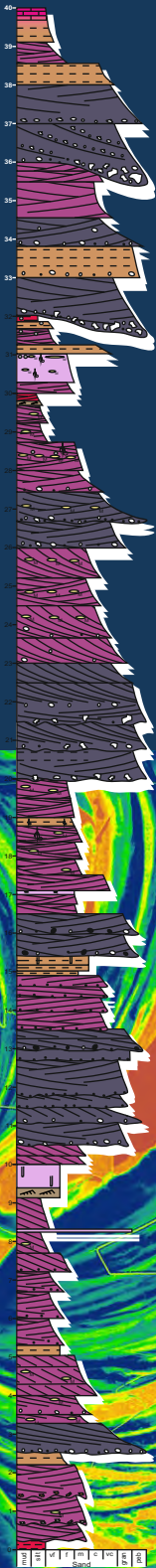


PB-SAND: Point-Bar Sedimentary Architecture Numerical Deduction

PB-SAND is a numerical forward stratigraphic model for the reconstruction and prediction of the spatio-temporal migratory evolution of fluvial and tidal meanders and their generated deposits that accumulate as heterogeneous sedimentary successions. The model uses a combined process-based, geometric, and stochastic approach.



- develop 3D quantitative facies models for high-sinuosity fluvial & tidal channel systems;
- model complex bar evolution arising from bar expansion, rotation and translation;
- predict the distribution of lithofacies within large barforms using rule-based methods;
- model internal heterogeneities & baffles arising from mud drapes on bar fronts;
- analyse sand proportion & connectivity in stacked & overlapping point-bar elements;
- predict the basin-scale 3D distribution of bar elements in tectonically active basins;
- instruct & constrain forward stratigraphic models and 3D geocellular models for enhanced characterization of subsurface fluvial & tidal successions.



Meander-belt deposits
Mississippi River (USGS/NASA)

PB-SAND: A Stratigraphic Model to Predict 3D Facies Arrangements Associated With Sinuous Fluvial and Tidally Influenced Channel Evolution

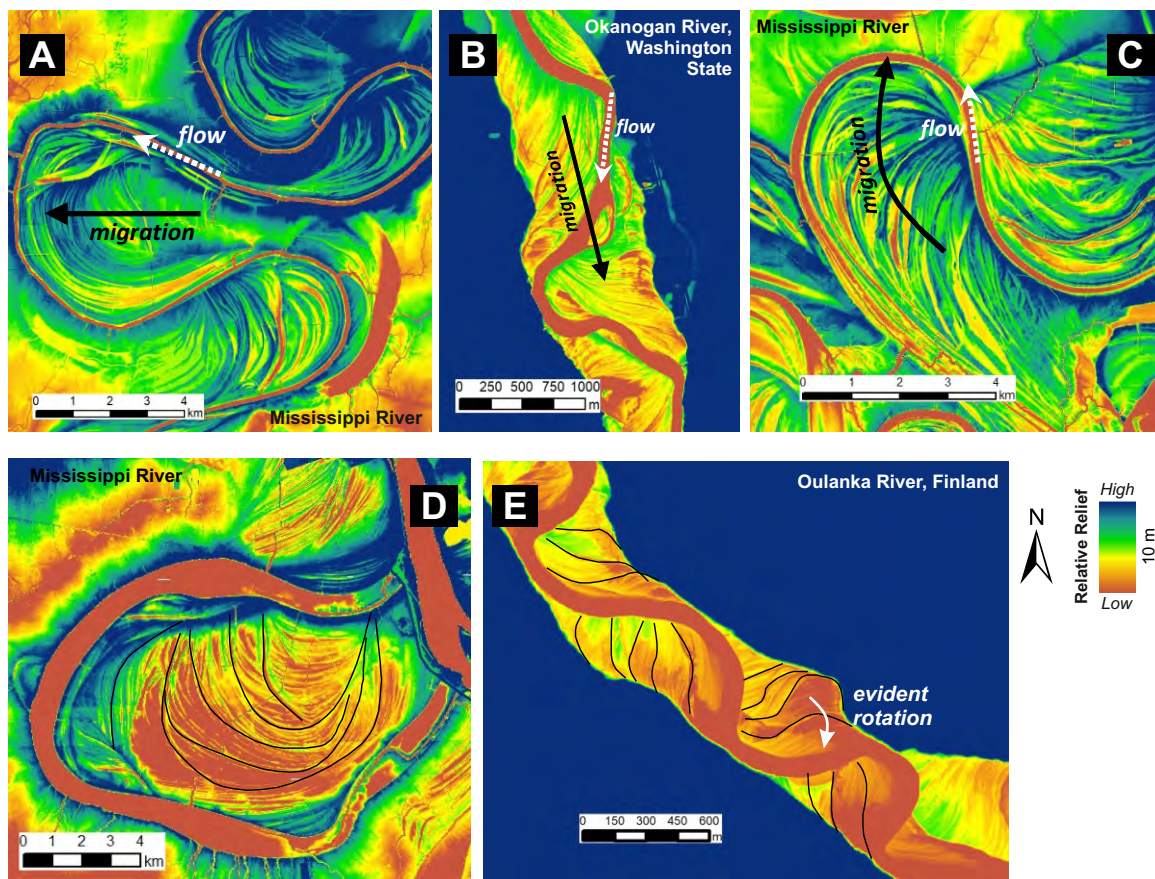
PB-SAND (*Point-Bar Sedimentary Architecture Numerical Deduction*) is a numerical forward stratigraphic model for the reconstruction and prediction of the complex spatio-temporal migratory evolution of fluvial and tidal meanders, their generated bar forms, and the associated lithofacies distributions that accumulate as heterogeneous sedimentary successions. PB-SAND uses a combined process-based, geometric, and stochastic modelling approach. The modelling approach integrates quantified sedimentological data from real-world case-study examples stored in a relational database, the Fluvial Architecture Knowledge Transfer System (FAKTS). The model predicts the internal architecture and geometry of point-bar, counter point-bar and related elements in three dimensions. The model is used to characterize subsurface reservoirs.

Sinuuous, meandering, channels characterize the lower reaches of many fluvial systems and some tidally influenced systems. Although fundamental types of meander-bend transformations have been recognized (expansion, translation, rotation, and combinations thereof), the relationships between the migratory behaviour of a river and the geometry and lithofacies organization of deposits that arise from channel migration (e.g. point bars and counter point-bars) remain relatively poorly understood.

Stratigraphic successions of fluvial depositional elements are commonly characterized by vertical and lateral facies heterogeneity that is indicative of highly variable mechanisms of accretion. Sand-prone packages are draped and partitioned by mud-prone deposits of variable thickness and continuity. Furthermore, at a larger scale, the morphology and preserved lithofacies of meander belts is influenced by both autogenic factors, such as frequency of nodal avulsion, and allogenic factors, such as climate-driven changes in sediment delivery and the role of differential subsidence in controlling direction and rate of meander-belt migration.

Benefits of PB-SAND:

- (1) Flexibility to control meander-bend migration rates and morphology without the need to account for complicated hydraulic processes;
- (2) Capability to incorporate independent geomorphic controls (e.g., valley confinement);
- (3) Ability to constrain the model output using parameters derived directly from empirical field measurements and remote sensing;
- (4) Ability to directly compare modelling outcome with real-world datasets derived from outcrops or boreholes;
- (5) High computational efficiency.



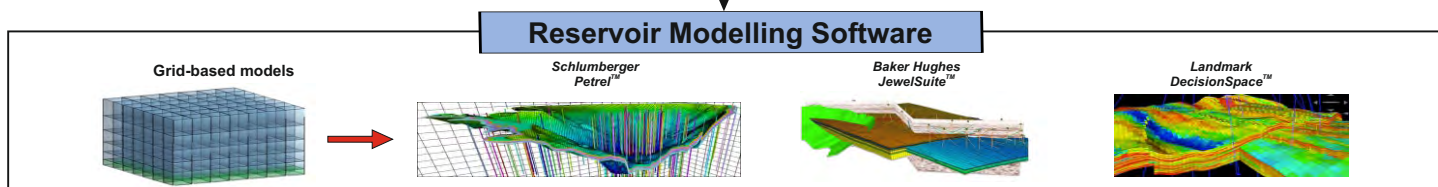
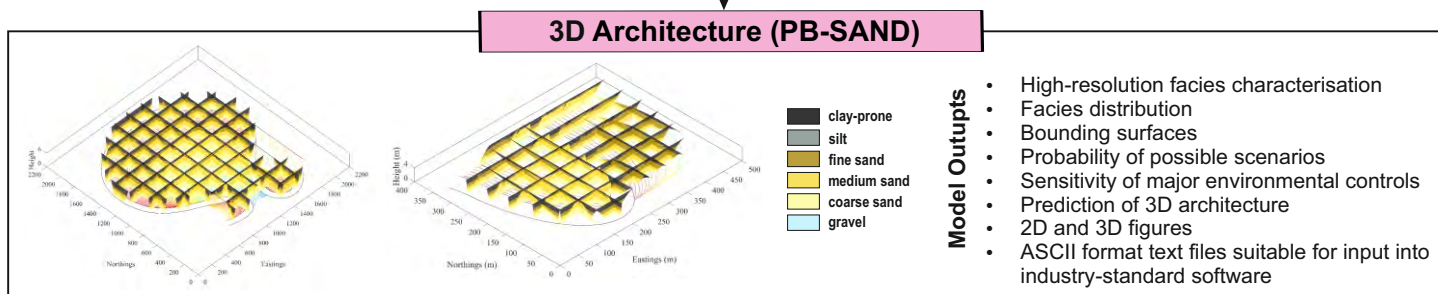
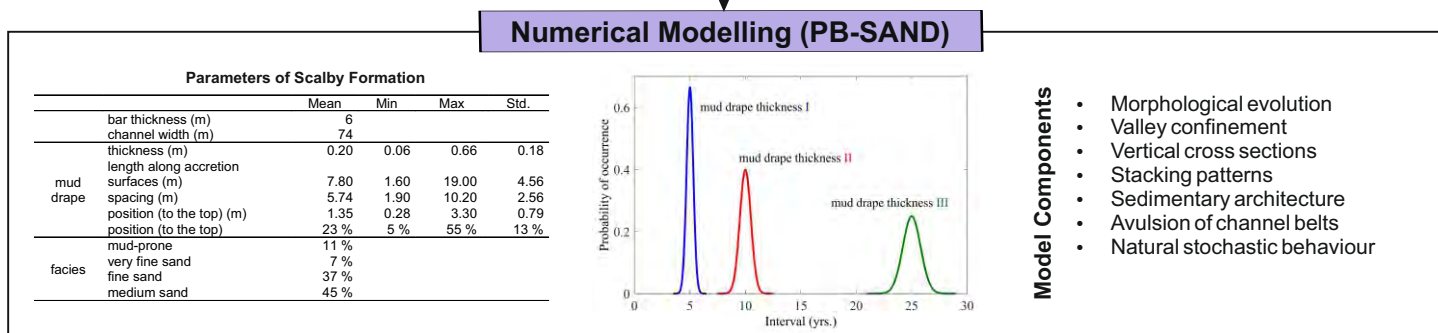
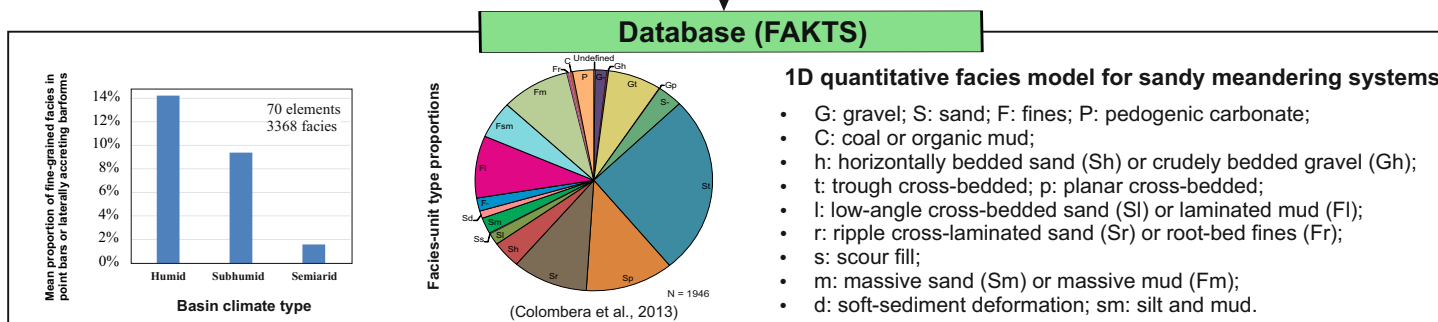
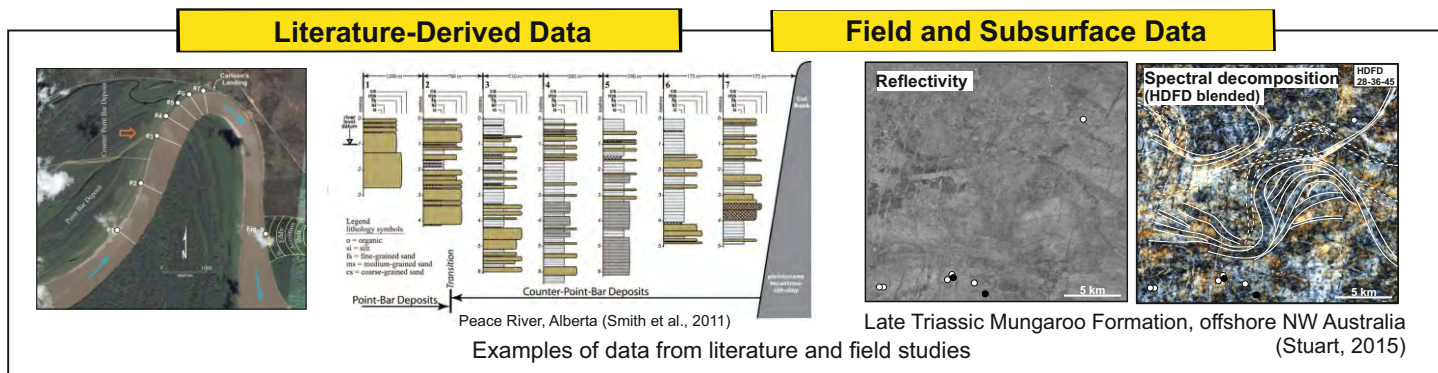
Left. (A) Typical point-bar example developed by lateral migration with minor apex rotation. (B) Typical point-bar example developed by downstream migration. (C) Point-bar example developed by lateral migration combined with constant apex rotation. (D) Point-bar example developed through apex rotation that changes in sharp direction multiple times. Black lines denote boundaries of sedimentary packages. See erosive boundaries caused by changes in the direction of apex rotation. (E) Downstream translating point bar with evident apex rotation.

PB-SAND

Fluvial, Eolian & Shallow-Marine Research Group

<http://frg.leeds.ac.uk/>

PB-SAND: Integrated Numerical Modelling Approach and Workflow



PB-SAND can be employed to generate training-image libraries for use with MPS reservoir modelling workflows.

PB-SAND: User-Defined Modelling Parameters

Modelling Inputs

<p>single point bar</p> <ul style="list-style-type: none"> point bar transformation style coordinates of bar positions at three key times (x, y) migration rates ($m\ yr^{-1}$) or bar numbers ($\#\ m^{-1}$) between key times number of controlling point for each bar position river width (m) neck cutoff threshold (m) 	<p>multiple point bars</p> <ul style="list-style-type: none"> percentage of different bar transformation styles orientation distribution curve ($^{\circ}$, unimodal or bimodal) size distribution curve point bar longevity control (time or cut-off) point bar density distribution in a channel belt width of channel belt (m) spatial distribution curve of channel belts avulsion frequency of channel belts (yrs) spatial change of subsidence rate, e.g., faults ($m\ yr^{-1}$) tectonic boundaries if existing
<p>channel asymmetry & shape of accretion surfaces</p> <ul style="list-style-type: none"> river width (m) bar depth (m) dip angle ($^{\circ}$) maximum deposition rate of inner bank ($m\ yr^{-1}$) maximum erosion rate of cut bank ($m\ yr^{-1}$) maximum wavelength of inclined accretion surface (m) minimum wavelength of erodible slope (m) 	<p>mud drapes on bar-front surfaces</p> <ul style="list-style-type: none"> probability distribution curves of 1-3 different levels of mud drapes <ul style="list-style-type: none"> thickness (m) minimum occurrence interval (yrs) maximum occurrence interval (yrs) shape factor of Gaussian distribution curve for interval position of mud drapes on bar front <ul style="list-style-type: none"> upper limit of mud drape front relative to bar depth lower limit of mud drape front relative to bar depth shape factor of Gaussian distribution curve for position continuity of mud drapes in cross sections <ul style="list-style-type: none"> maximum numbers (1-3) of gaps within a mud drape size of gap relative to bar depth upper boundary of the gap position relative to bar depth lower limit of the gap position relative to bar depth probability of occurrence of 1-3 gaps shape factor of Gaussian distribution curve for gap position continuity of mud drapes in plan view <ul style="list-style-type: none"> minimum length of mud drapes (m) maximum length of mud drapes (m) shape factor of Gaussian distribution curve for length minimum length of spacing (m) maximum length of spacing (m) shape factor of Gaussian distribution curve for spacing
<p>location of cross sections</p> <ul style="list-style-type: none"> cross section area <ul style="list-style-type: none"> width (m) length (m) coordinates of centre (x, y) degree of clockwise rotation ($^{\circ}$) resolutions of cross sections in width (m) and length (m) 	<p>Channel lag deposits (conglomerate & breccia)</p> <ul style="list-style-type: none"> probability distribution curves of 1-3 different levels of conglomerates or breccias <ul style="list-style-type: none"> thickness (m) minimum occurrence interval (yrs) maximum occurrence interval (yrs) shape factor of Gaussian distribution curve for interval uppermost position of conglomerates or breccias on bar front <ul style="list-style-type: none"> upper boundary relative to bar depth lower boundary relative to bar depth shape factor of Gaussian distribution curve for position
<p>facies associations</p> <ul style="list-style-type: none"> point bar transformation style facies types proportions of different facies at representative point-bar locations <ul style="list-style-type: none"> early stage expansional point bar mature stage and high sinuosity expansional point bar transitional zone between early and later stages of expansional point bar counter-point bar by downstream translation transitional zone between point bar and counter-point bar apex portion by translation and rotation proportions of different facies in abandoned channels 	
<p>shape of facies unit bounding surfaces</p> <ul style="list-style-type: none"> inclination for each bounding surface <ul style="list-style-type: none"> minimum and maximum degree of inclination ($^{\circ}$) minimum and maximum years of a cycle (m) shape factor of Gaussian distribution curve for cycling years disorder and randomness level for each bounding surface <ul style="list-style-type: none"> disorder level, in percentage of to bar depth minimum and maximum years of a cycle (m) shape factor of Gaussian distribution curve for cycling years 	

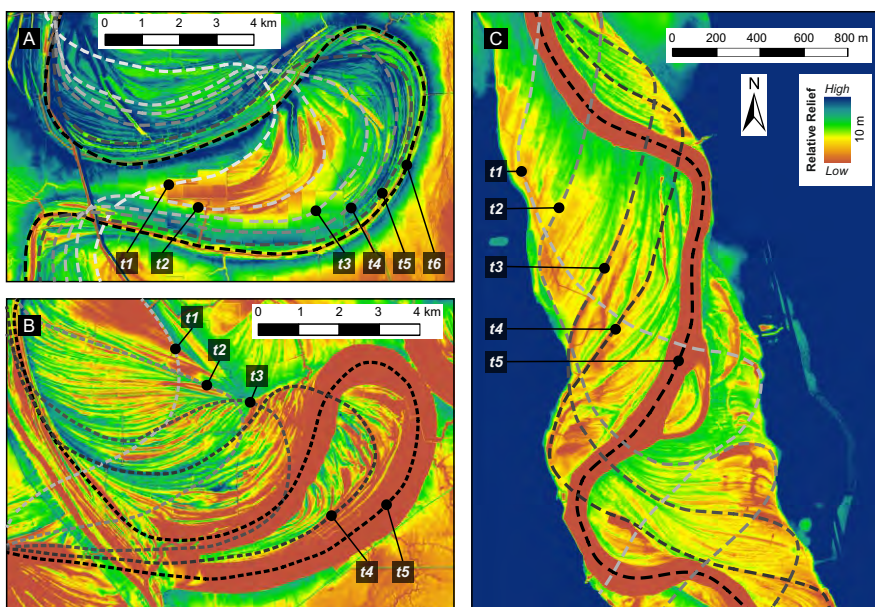
Modelling Outputs

<ul style="list-style-type: none"> high resolution plan-view morphology facies distribution in 3D bounding surface geometries (2nd order) mud drapes at different scales (3rd order) multiple point-bar elements in a meander belt multiple meander belts 	<ul style="list-style-type: none"> stacking patterns and connectivity change caused by different subsidence rates and avulsion rates sensitivity of parameter controls cross sections training images for MPS 3D fence diagrams ACSII txt. format output files
---	---

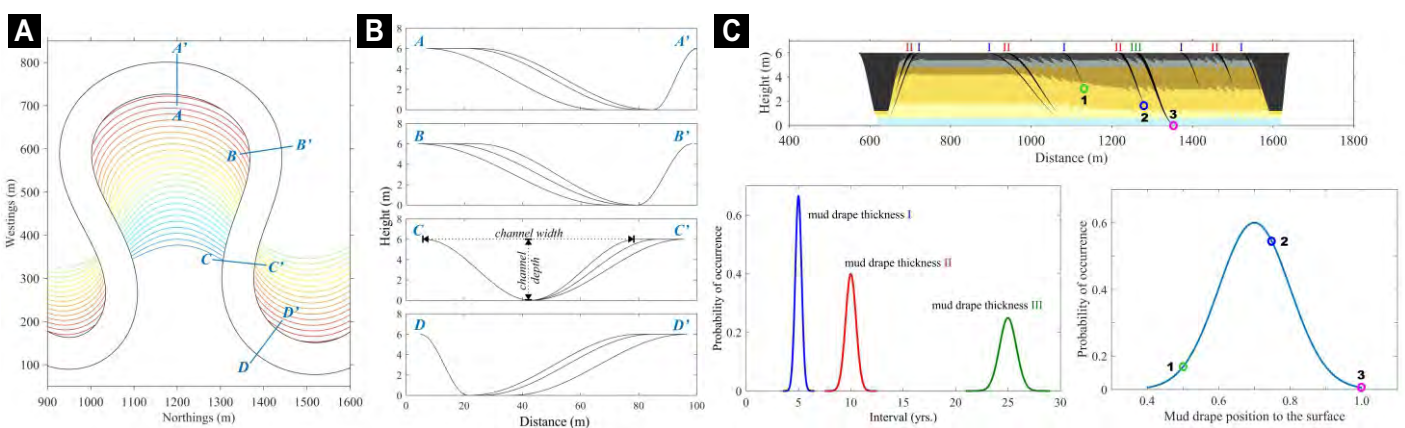
PB-SAND: Approach to Modelling Point-Bar Evolution in 3D

PB-SAND is able to reconstruct and predict the three-dimensional sedimentary architecture arising in response to different types of channel migration at varying temporal and spatial scales under unrestricted horizontal and vertical resolutions by virtue of its vector-based modelling technique. PB-SAND can model planform evolution of one or several point-bar elements, and can also model the facies distribution present in vertical sections at any position through the point bar. Three-dimensional model output can be expressed as plan view slices or cross sections made in any orientation. The model predicts the arrangement of lithofacies according to data derived from natural examples stored in FAKTS.

- Model the complex, multistage planform evolution of point-bar elements.
- Reveal stratal architectures of point-bar elements and facies arrangements of vertical sections.
- Model and output facies distributions of point-bar elements in three dimensions.
- Model bar thickness variations caused by thalweg bathymetric change.
- Incorporate climbing trajectories for systems influenced by river aggradation and migration.
- Model the spatial distribution (continuous or discontinuous) of bar-front mud drapes and gravel lags associated
- Model PB vertical stacking & partial overprinting.



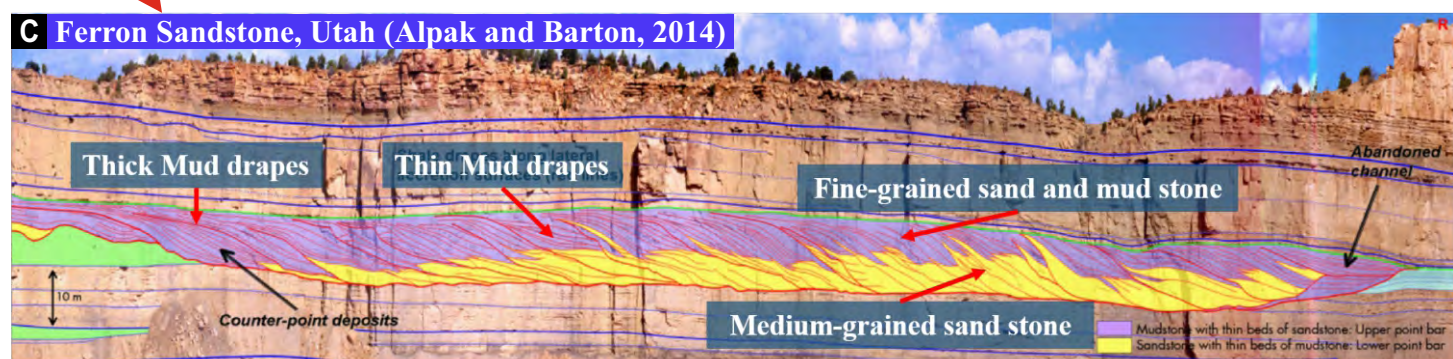
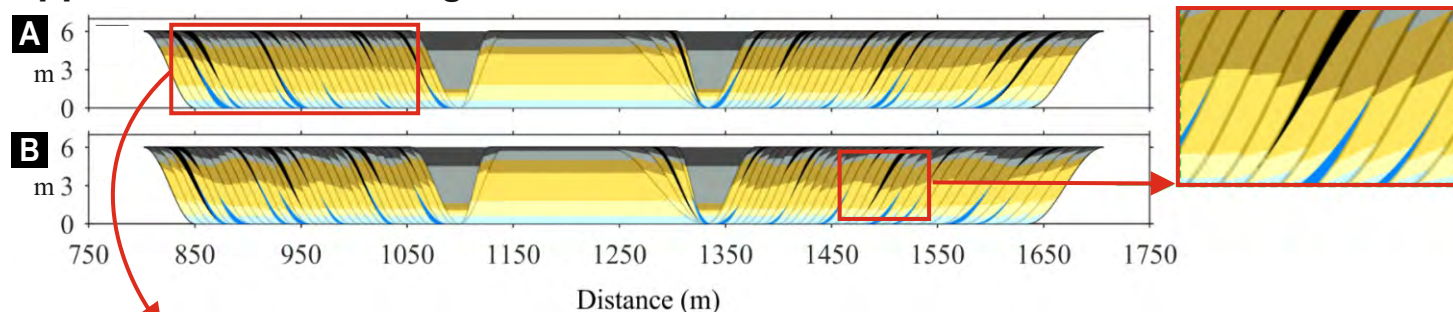
Left. Example of input trajectories used as input to PB-SAND for modelling planform evolution of meander bends. Input trajectories representing the centrelines of channels are assigned a relative chronological order and shown as dotted lines. Both point bar A and point bar B experienced a marked lateral expansion, and the point bar B (t1 vs. t5) undertook a substantial rotation of the meander-bend apex as compared with the point bar A (t1 vs. t6). In contrast, the development of point bar C is predominantly controlled by downstream translation with minimal lateral migration and bend-apex rotation. Digital elevation data courtesy USGS. Meander evolution can be modelled from knowledge of as few as three former channel paths; more complex bend evolution requires knowledge of additional channel paths. Such paths may be determined from seismic stratal slices.



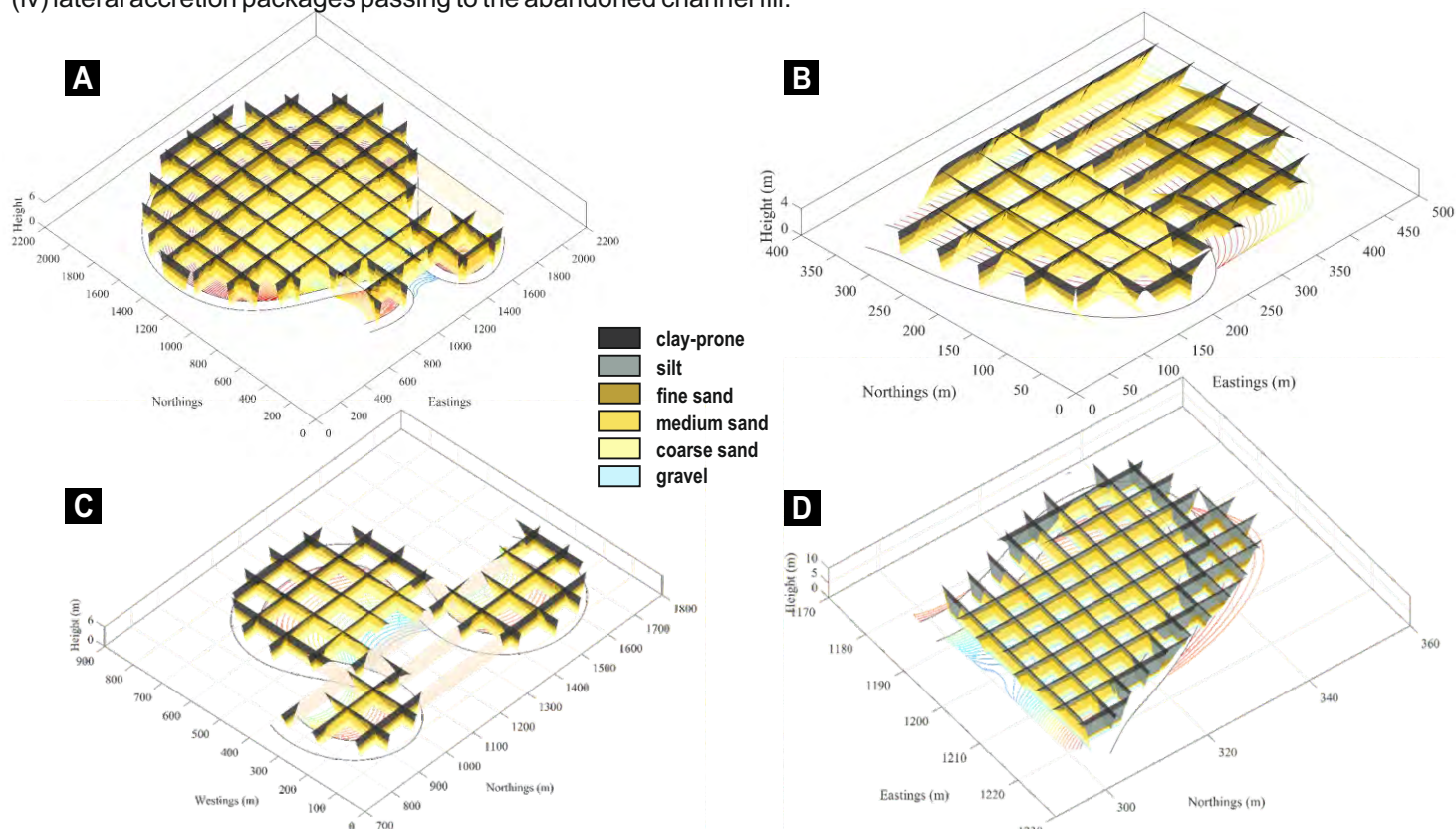
Above. (A) PB-SAND modelling example for a typical expansional point bar. (B) Channel-bank profiles of representative cross sections. (C) Examples of modeling multiple-scale mud drapes with three different thicknesses (I, II and III) that are controlled by their respective probability curves of occurrence. The vertical position of the point to which mud drapes extend down the bar front are also modelled using a Gaussian distribution curve specified by users; three examples are shown in circles. See details in Yan et al. (2017, 2018).

PB-SAND

Application 1: Modelling Individual Point-Bar Elements & Internal Lithofacies



Above. Comparison of modelled cross-section examples (A & B) with an outcrop (C) of Ferron Sandstone in Utah, USA. The modelled cross sections can mimic outcrops seen in the real-world: (i) fining-upward facies distribution within the point bar; (ii) thinner mud drapes occur more frequently than thicker mud drapes; (iii) natural fluctuation of the proportions of different facies; (iv) lateral accretion packages passing to the abandoned channel fill.

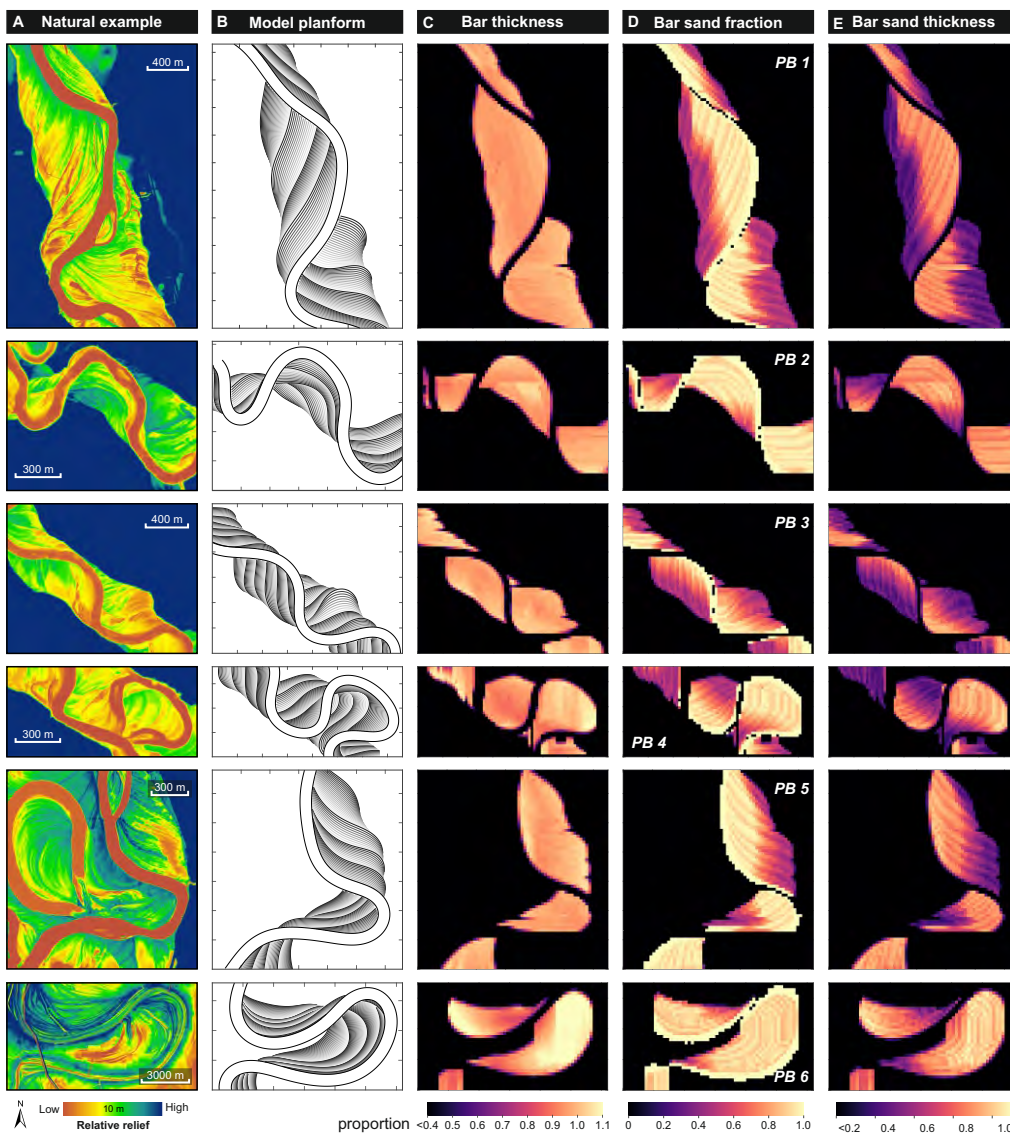


Above. Modelled examples of point-bar elements developed by different meander-bend transformation styles. (A) High-sinuosity expansional point bar. (B) Downstream translating point bar. (C) Low-sinuosity expansional point bar. (D) Downstream translating and rotating point bar. Fence diagrams of cross-lines and in-lines superimposed on plan forms.

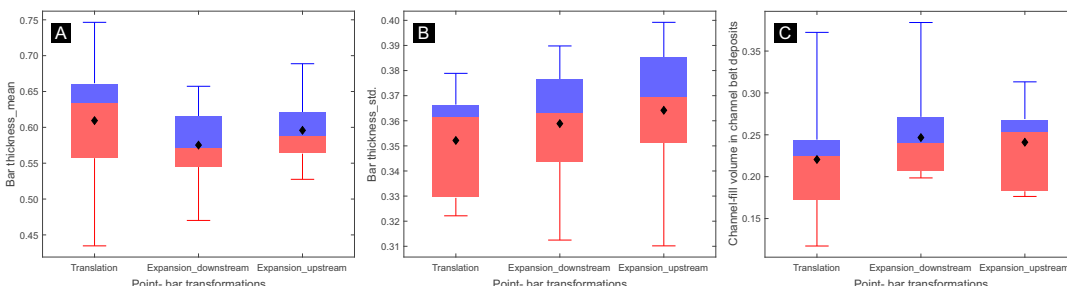
Application 2: Prediction of Lithological Heterogeneity, Bar Thickness, Bar Sand Proportion & Bar Sand Thickness

PB-SAND can model 3D architecture and lithofacies distributions of point bars with different planform morphology and scroll-bar patterns that arise from their unique bar growth history associated with the style and magnitude of meander transformation and bend-apex rotation. The modelled outputs can be used to quantify the relationships between point-bar

planform evolution and associated facies heterogeneity, bar geometry, and sand volume. The tool can be used to predict sand distribution and volume in point-bar deposits based solely on information about the planform morphology and scroll-bar patterns that might typically be observable in seismic stratal slices. Predictions of sand occurrence & quality are made in pre-drill settings.



Left. Point bar examples depicting different types of meander-transformation style, embodying different combinations of expansion, translation, and rotation of varying degrees. Based on high-resolution LiDAR images (A), planform morphology of point-bar sections (B) are modelled by PB-SAND. Bar thickness (C) are modelled to mimic the development of progressively deeper pools near meander-bend apices and progressively shallower riffles centred on the meander inflection points. The sand fraction and sand thickness are modelled by imposing various rules that follow geological understanding of facies change trends around meander bends, including (i) fining-upward trends with mud deposits on the bar top and sand deposits beneath, (ii) downstream fining beyond the preserved expression of the meander apex, and (iii) progressive transition from point-bar to counter-point-bar deposits. This approach to modelling can be used to predict sand distribution and quality in pre-drill settings using only limited data from low-resolution seismic stratal slices.

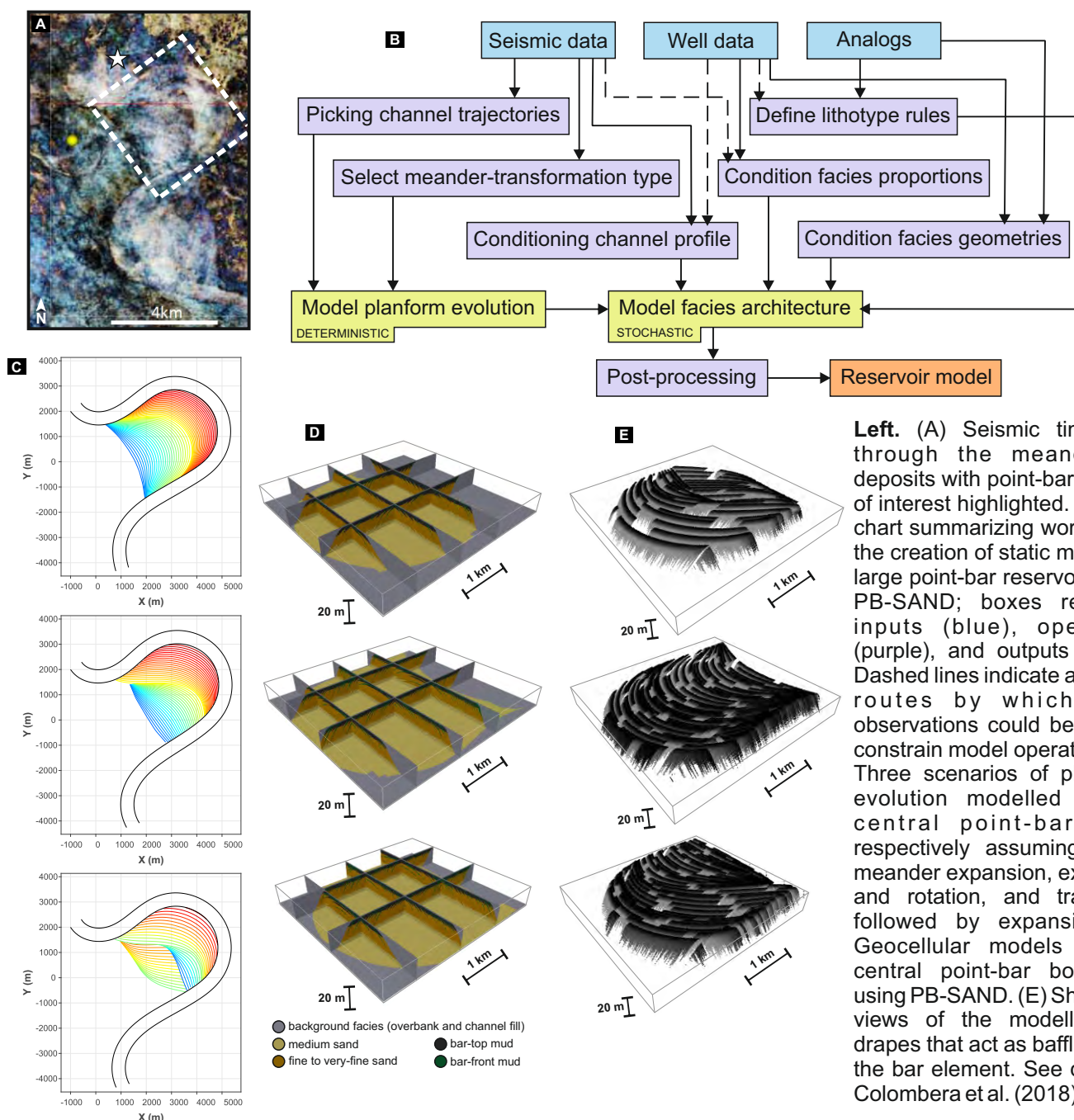


Left. Box plots of bar thickness (A), their standard deviation (B), and channel-fill volume in channel belt deposits (C) categorized by the transformation styles of point-bar development.

Application 3: Prediction of Extent and Continuity of Mud Drapes That Act as Flow Baffles for Improved Geocellular Modelling of Meander-Belt Reservoirs

PB-SAND can use information from seismic interpretations to predict realistic facies distributions in high-resolution geomodels of point-bar reservoirs. PB-SAND permits the integration of subsurface data with insight gained from geologic analogs. The modelling tool uses knowledge of sedimentological processes to determine lithologic organization through a rule-based approach, to explore different scenarios of point-bar reservoir architecture for

development purposes. Constructing point-bar reservoir models using PB-SAND permits a more direct control on the reproduction of geologic features that are important in affecting the static connectivity of net-reservoir volumes (distribution and characteristics of mud drapes, mud-prone packages), compared to traditional variogram-based methods.



PB-SAND

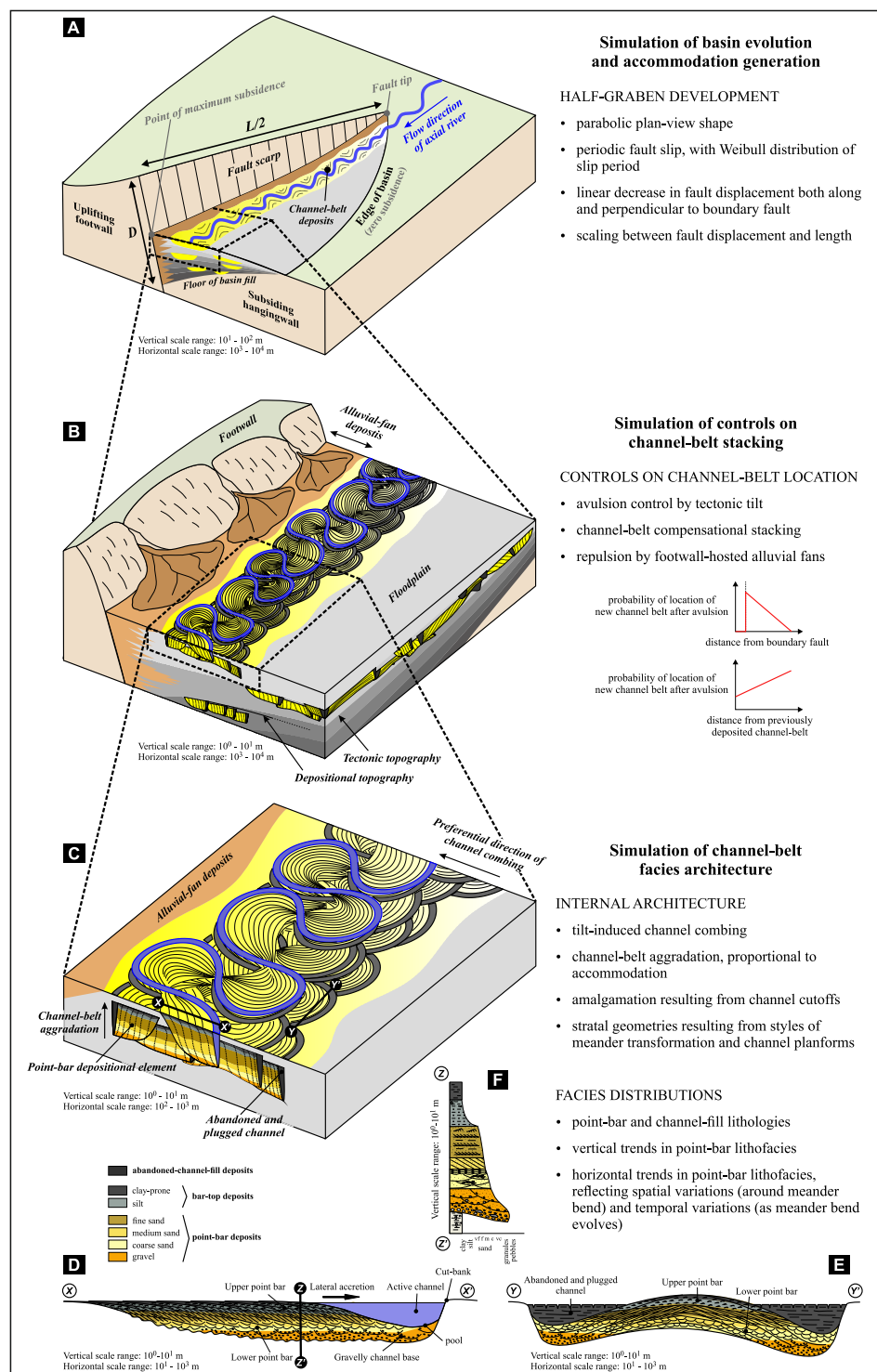
Fluvial, Eolian & Shallow-Marine Research Group

<http://frg.leeds.ac.uk/>

Application 4: Determine Sandbody Distribution & Connectivity in Tectonically Active Basins With Complex Subsidence and Sediment Fill Histories

The spatial organization of meandering-river deposits varies greatly within the sedimentary fills of rift-basins, depending on how differential rates of fault propagation and subsidence interplay with autogenic processes to drive changes in fluvial channel-belt position and rate of migration, avulsion frequency, and mechanisms of meander-bend cut off.

This process fundamentally influences stacking patterns of the accumulated successions. PB-SAND can be used to reconstruct and predict the complex morphodynamics of fluvial meanders, their generated bar forms, and the associated lithofacies distributions that accumulate as heterogeneous fluvial successions in rift settings. Modelling can be constrained by data from seismic images and wells.

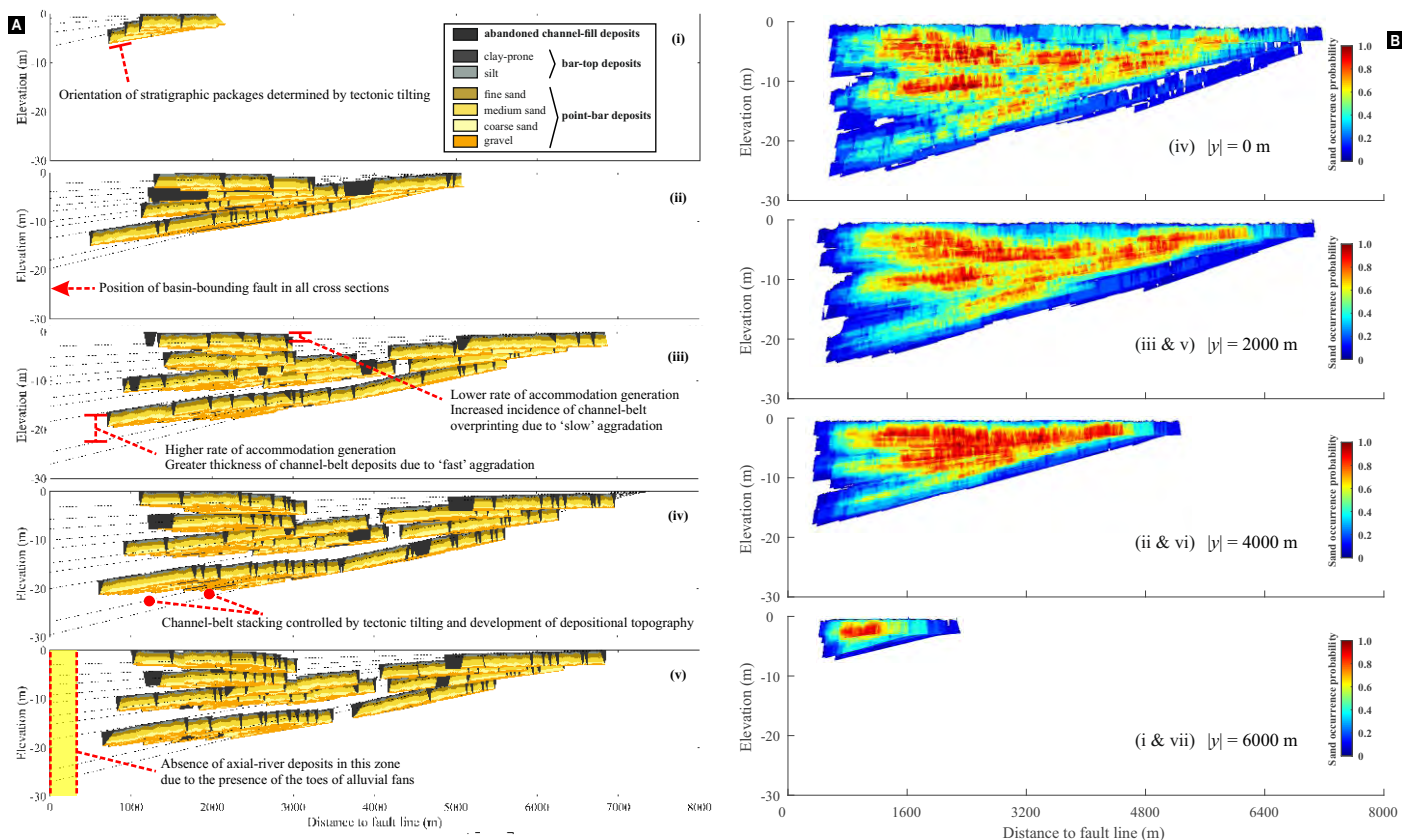


Left. Schematic diagram of an evolving half-graben basin in a fluvial-dominated continental setting. (A) Section through part of a half-graben basin. An axial river runs through the basin close to the line of the fault. L is the length of the fault. D is the accumulative displacement. (B) Stacking of channel-belt deposits that are controlled by the generation of accommodation and the presence of a surface gradient induced by tectonic tilting. (C) Architecture of channel-belt deposits. Controlled by tectonic tilting, axial rivers tend to migrate toward the fault zone within an evolving rift basin, resulting in preferential preservation of older abandoned channel-fill elements in an up-tilt direction. (D) A representative cross section in the transverse direction of a channel-belt accumulation. (E) A representative cross section in a direction parallel to the trend of the channel-belt. Typical fining-upward lithofacies successions are shown in the cross sections. (F) Typical grain-size profile of a vertical cross section of a point-bar deposit. Note vertical scales are highly exaggerated. D-F modified in part from Ghazi and Mountney (2009). See details in Yan et al. (2020). The 3D modelling outputs can be used to explore the spatial variability in the size and connectedness of sand-prone geobodies as a function of the interaction between spatial and temporal variations in rates of accommodation generation and fault-influenced changes in river morphodynamics.

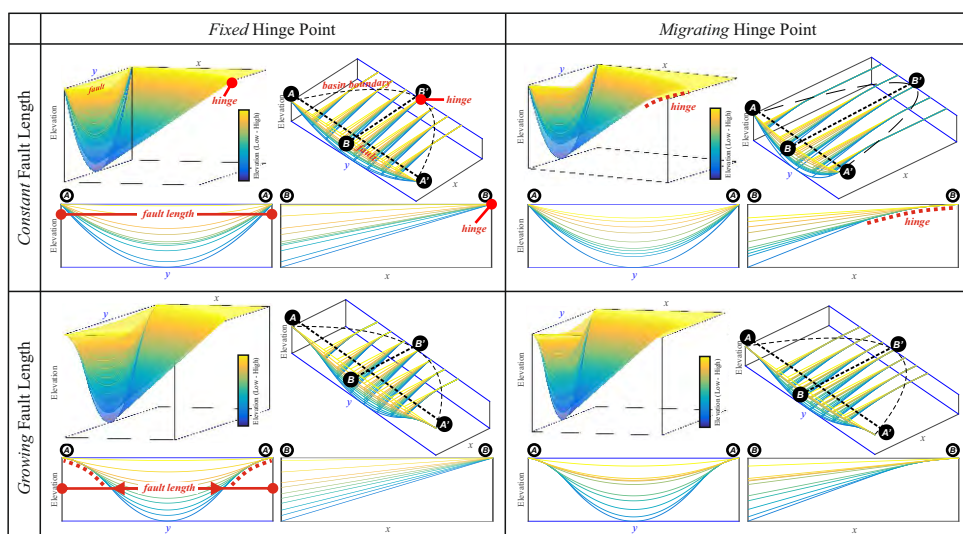
PB-SAND

Fluvial, Eolian & Shallow-Marine Research Group

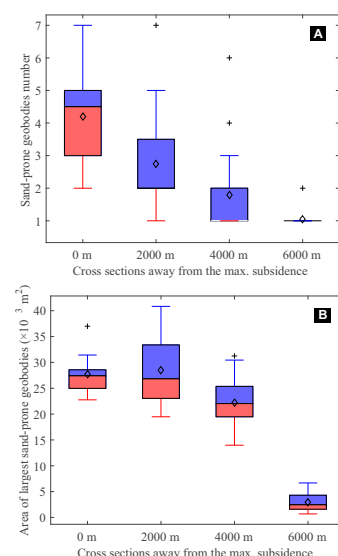
<http://frg.leeds.ac.uk/>



Above. (A) Example of modelled stratigraphic cross sections (perpendicular to fault trend) after 10 episodes of basin-fill aggradation and channel avulsions induced by tectonic tilting of a half-graben basin. The black dotted lines denote the floodplain surface at the time tectonic tilting and associated triggered avulsion events occur. Model results show how the connectivity of point-bar elements changes through the basin and with varying proximity to the bounding fault by different subsidence rates induced by tectonic tilting. (B) Cross-sectional maps of the probability of sand or gravel occurrence using cross sections from all ten simulations. The resolution is 8 m in the horizontal direction and 0.5 m in the vertical direction.



Above. Different evolution styles of individual fault-bounded half-graben basins, from PB-SAND modelling examples. The development of individual faults is induced by episodic slip events. The ten most recent stratigraphic intervals representing the accommodation generated by tectonic events are shown in 3D and frame diagrams. Cross sections A-A' and B-B' in each of the four cases show subsidence change parallel and perpendicular to the fault, respectively. The graded colour denotes fault boundaries by each slip event. As subsidence increases, a basin changes shape depending on how the fault grows laterally and how the hinge point of the hangingwall rollover migrates away from the fault.



Above. (A) Box plots of the distribution in the number (A) and in the area of largest (B) of sand-prone geobodies of cross sections perpendicular to the fault in a half-graben basin.

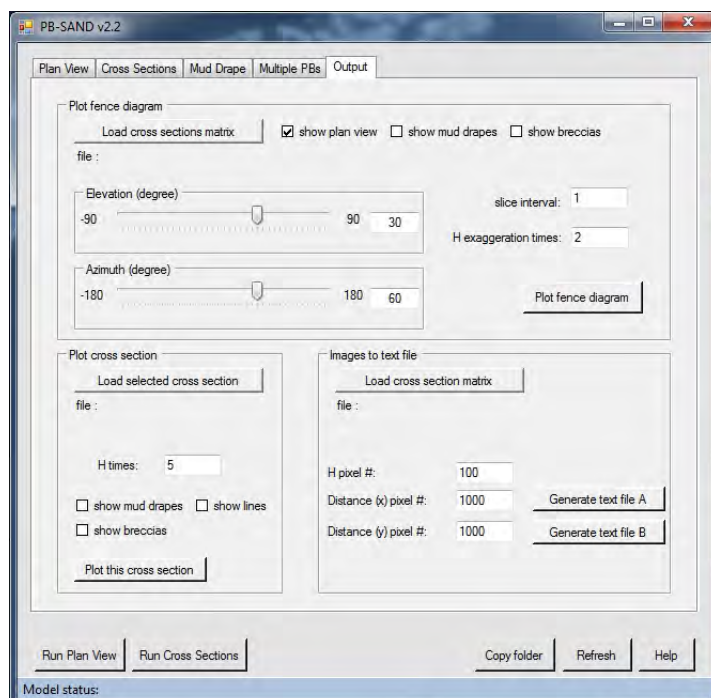
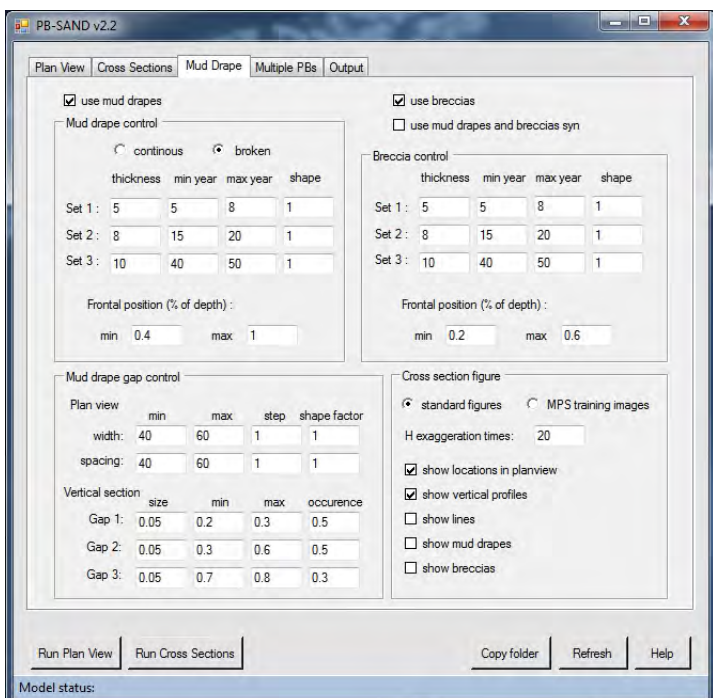
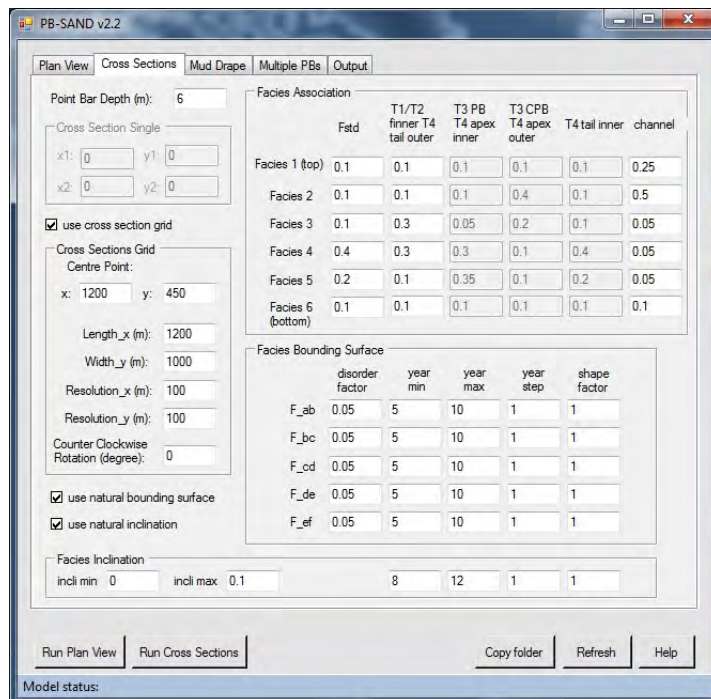
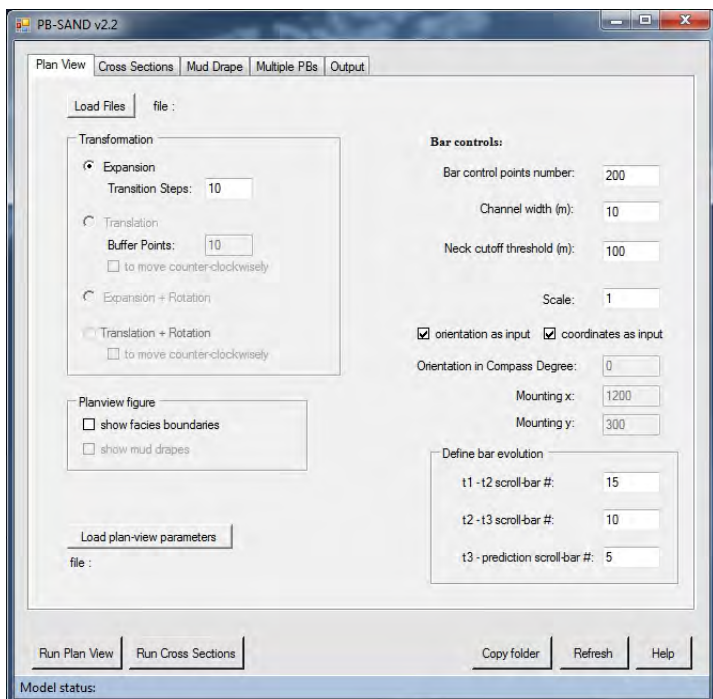
PB-SAND

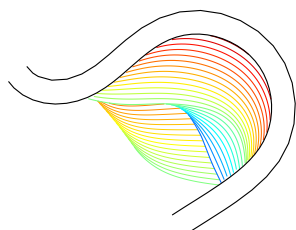
Fluvial, Eolian & Shallow-Marine Research Group

<http://frg.leeds.ac.uk/>

PB-SAND: Programming Interface

PB-SAND is being developed as a research tool. The software has a simple user interface, and is able to model point-bar elements developed by different transformation styles: expansion, translation, rotation and the combinations thereof. PB-SAND can model different lithological characteristics associated with meander-bend transformation behaviours, e.g., counter-point-bars associated with down-stream translation, and finer facies associated with an increase of sinuosity. PB-SAND can model different thickness, continuity, spatial distribution, and temporal frequency of mud drapes and breccias within point-bar elements. The core modelling algorithm is vector-based and is therefore not restricted by resolution, as in raster-based models. Outputs from PB-SAND can be translated into ASCII format for use as input to standard industry software packages (e.g., Schlumberger Petrel) for reservoir modelling.

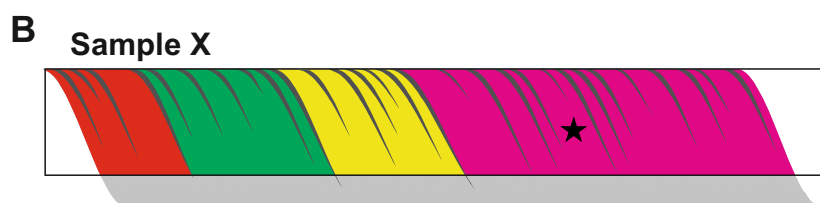
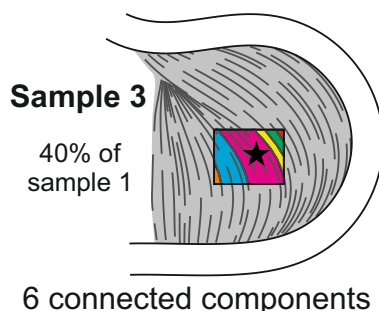
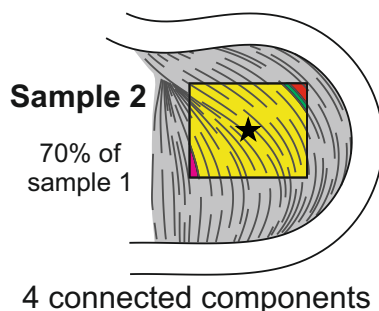
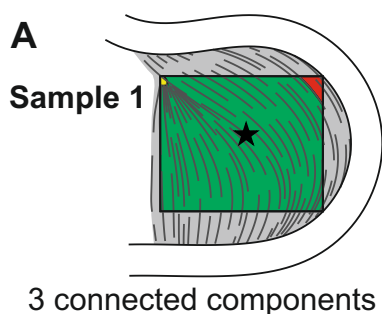




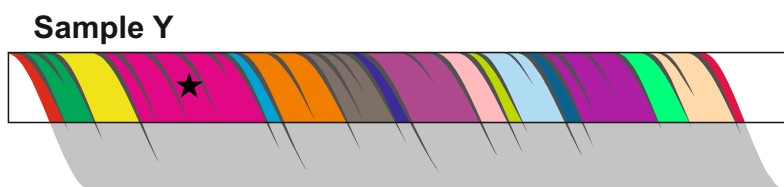
PB-SAND

Point-Bar Sedimentary Architecture Numerical Deduction

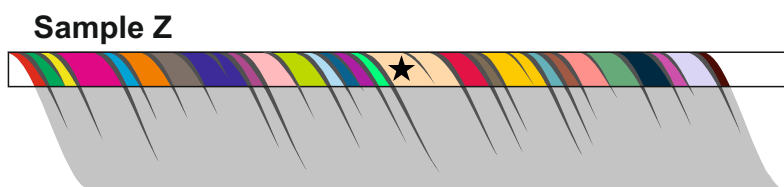
The **Point-Bar Sedimentary Architecture Numerical Deduction** is a modelling tool for the reconstruction and prediction of the complex spatio-temporal evolution of fluvial meanders, their generated 3D lithofacies distributions and resulting heterogeneity. The model permits the reconstruction of point-bar geometries and internal sedimentary architectures using a deterministic approach to simulate accretion patterns as they evolve over a series of time steps. The input trajectories that control the planform morphology of point bars can be digitized from seismic images, from remotely sensed images of modern systems, or devised based on field observations of ancient outcropping successions.



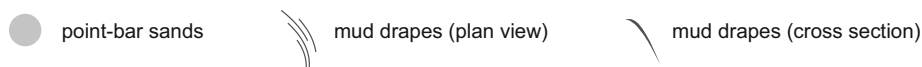
75% of bar thickness
4 connected components



50% of bar thickness
17 connected components



25% of bar thickness
27 connected components



Above. Idealized examples that illustrate the effect of sample size on the number and size of connected components made of point-bar sands that are compartmentalized by mud drapes, in both plan view (A) and cross sections (B). In each sample (black frames), different connected components of point-bar sands are represented as variably coloured sectors. The largest connected components in each sample are denoted by stars. Although these examples are depicted as two-dimensional sections, in reality all the metrics presented here result from 3D analysis. Analysis of the connectivity of point-bar sands in samples of variable planform and vertical extent allows assessment of the degree at which compartments and dead ends develop at different length-scales.